Supplemental Data. Liebminger et al. (2009). Class I α-mannosidases are required for N-glycan processing and root development in *Arabidopsis thaliana*.

A

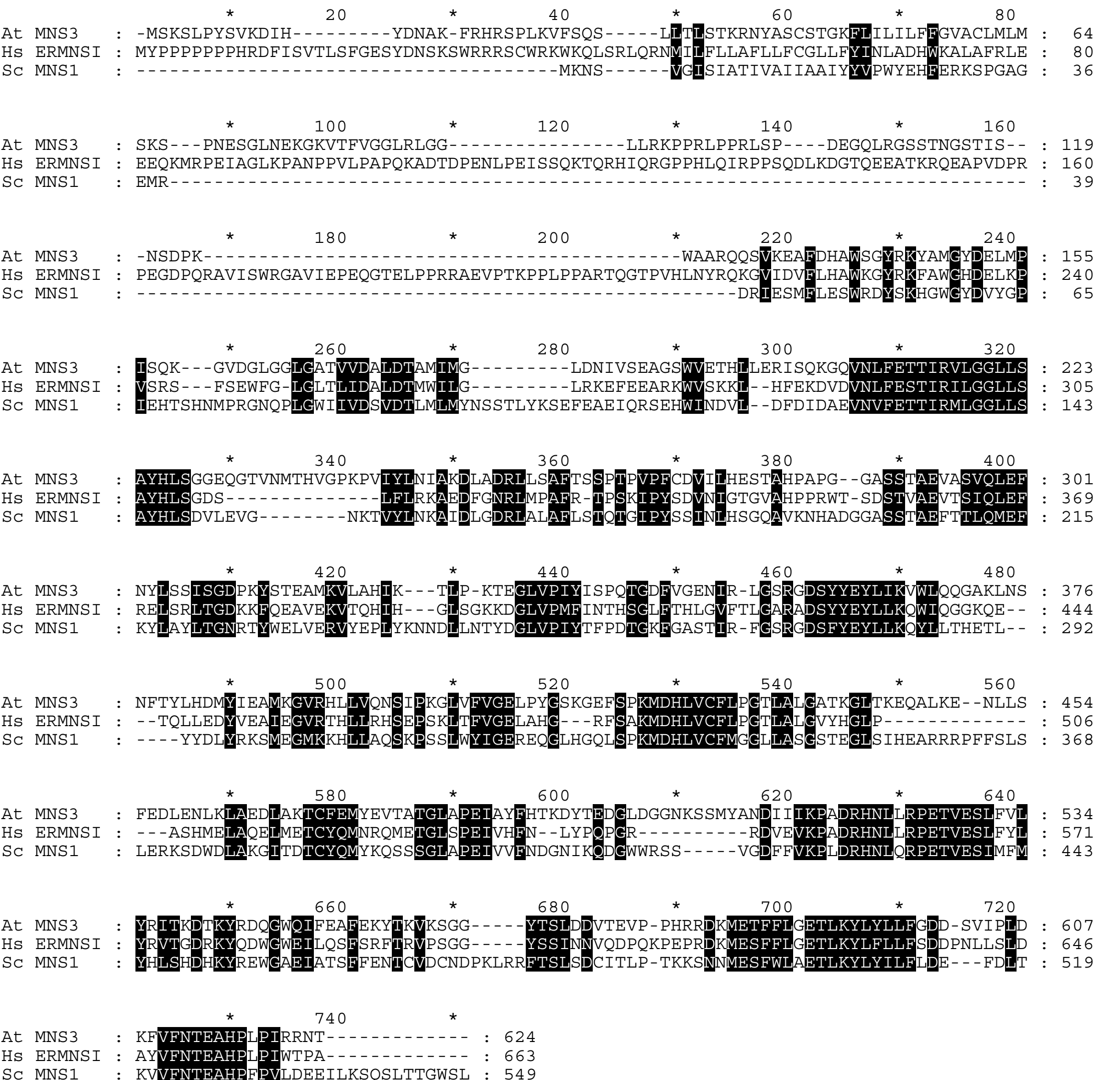

B

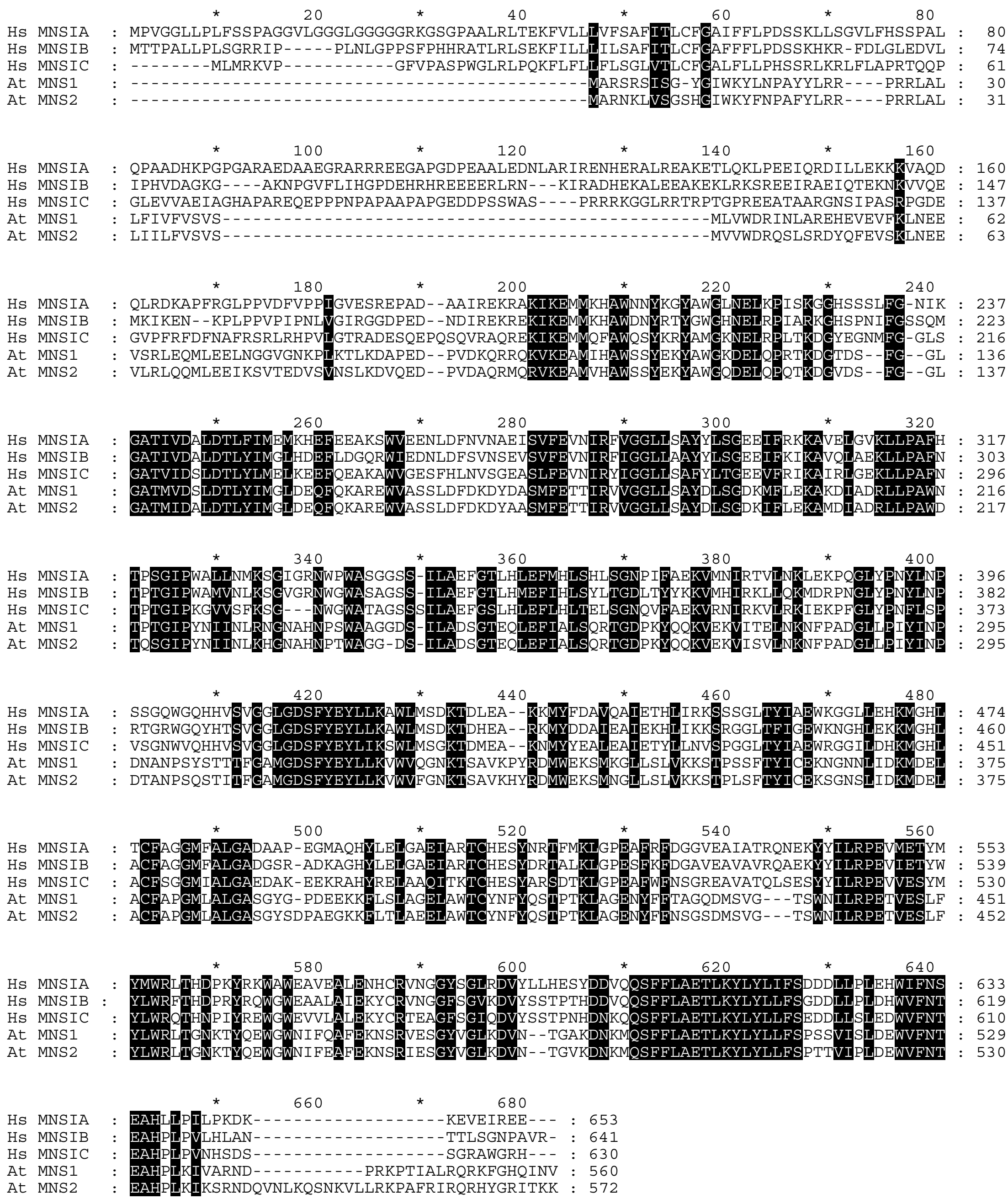

Supplemental Figure 1. Multiple sequence alignment of (A) At MNS3 with human (HsERMNSI) and yeast (ScMNS1) ER-MNSI proteins and (B) MNS1 and MNS2 with human Golgi-MNSIs (HsMNSIA-C). The sequence alignments were performed with ClustalW (http://www.ebi.ac.uk/Tools/clustalw2/index.html) and were edited manually. Conserved amino acid residues are shaded black. Dashed lines represent gaps inserted for optimal alignment of the sequences.

A

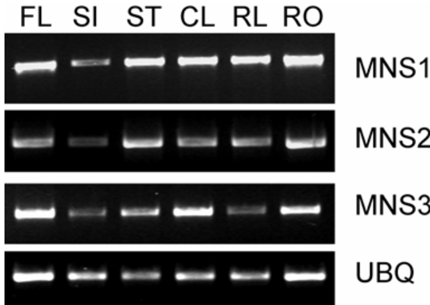

B

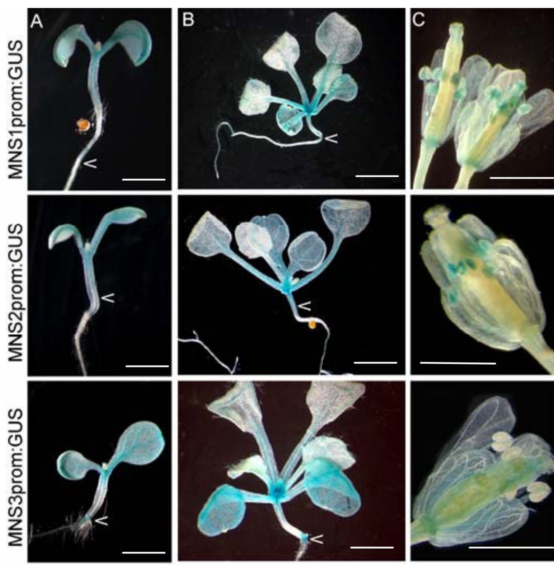

Supplemental Figure 2. Expression of MNS1, MNS2 and MNS3 in *Arabidopsis* tissues. (A) Reverse transcriptase-(RT)-PCR (two independent repeats) was performed using RNA extracted from flowers (FL), siliques (SI), stems (ST), cauline leaves (CL), rosette leaves (RL) and roots (RO). Specific primers were used for MNS1 (32 cycles), MNS2 (34 cycles), MNS3 (34 cycles) and UBQ (35 cycles) as control. The expression of the three α-mannosidase genes was detectable in all analyzed *Arabidopsis* organs, being consistent with a proposed constitutive expression of these genes. **(B)** Expression of promoter:β-glucuronidase (GUS) reporter constructs in *Arabidopsis*. The expression of $MNS1_{prom}$:GUS and $MNS2_{prom}$:GUS is almost indistinguishable, with high expression in pollen grains and shoot apical meristems of seedlings. $MNS1_{prom}$:GUS expression was also detected in hypocotyls and in the upper region of the root in young seedlings. $MNS3_{prom}$:GUS expression is detectable in

stamens and in sepals and in newly emerging rosette leaves. Arrow heads indicate subtle differences in the expression pattern of MNS proteins. Scale bar = 3 mm.

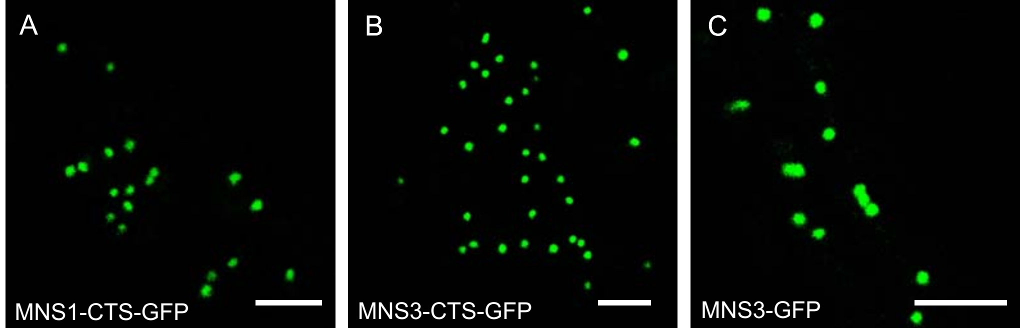

Supplemental Figure 3. MNS3-GFP is located in the Golgi apparatus of *Arabidopsis* cells.

A. thaliana seedlings expressing (**A)** MNS1-CTS-GFP, (**B)** MNS3-CTS-GFP and (**C)** MNS3-GFP were grown on MS medium plus 2% sucrose for four to seven days at 22°C. Seedlings were transferred onto microscope coverslips and were imaged on a Leica TCP SP2 confocal laser scanning microscope. GFP was imaged using a 488-nm argon laser line, and emission was recorded from 500 to 535 nm. **A-C:** MNS-GFP fusions are located in mobile punctate structures reminiscent of Golgi bodies. No ER labeling was observed. Scale bar = 5 µm.

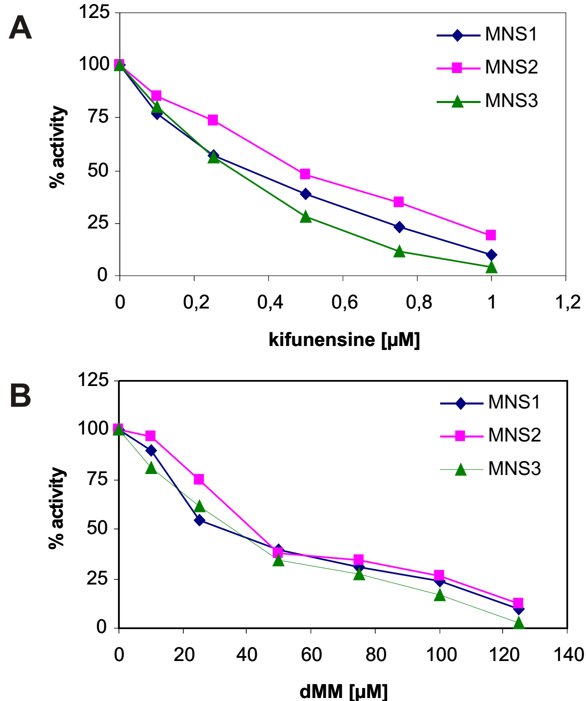

Supplemental Figure 4. Recombinant MNS proteins are specifically inhibited by kifunensine and 1-deoxymannojirimycin. Activity assays with methyl-2-O-α-D-mannopyranosyl-α-D-mannopyranoside as substrate were performed as described in Material and Methods. (**A)** Inhibition of MNS1-3 by kifunensine and **(B)** inhibition of MNS1-3 by 1-deoxymannojirimycin (dMM) expressed as a percentage of control activity in the absence of inhibitor.

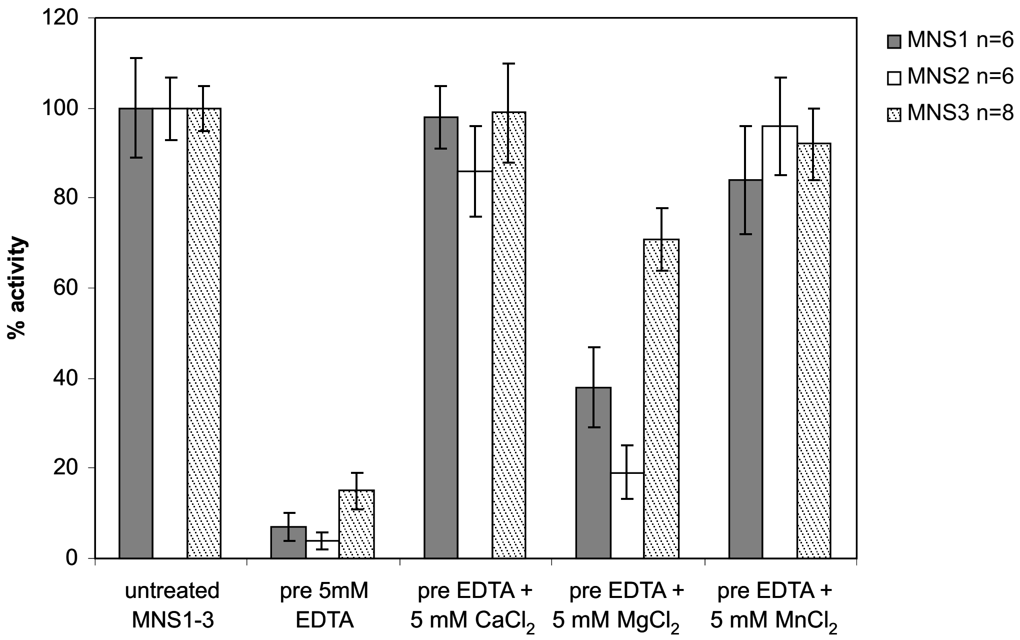

Supplemental Figure 5. **EDTA affects α-mannosidase activity of recombinant MNS proteins.** After incubation of MNS1-3 with 5 mM EDTA**,** methyl-2-O-α-D-mannopyranosyl-α-D-mannopyranoside was added. Activity assays were performed as described in Material and Methods. Restoration of enzyme activity was observed after addition of divalent cations.

		Elution position (Glc units)
		RP-HPLC
Man$_9$GlcNAc$_2$	Man9	5.33
Man$_8$GlcNAc$_2$	Man8.1	4.76
	Man8.2	6.40
	Man8.4	5.65
Man$_6$GlcNAc$_2$	Man6.1	6.15
	Man6.8	6.18
	Man6.10	7.82
Man$_5$GlcNAc$_2$	Man5.1	7.25

Supplemental Figure 6. **N-glycan structures relevant for this study.** The elution positions of each oligosaccharide on RP-HPLC are taken from the literature (Tomiya et al., 1991, Neeser et al., 1985).

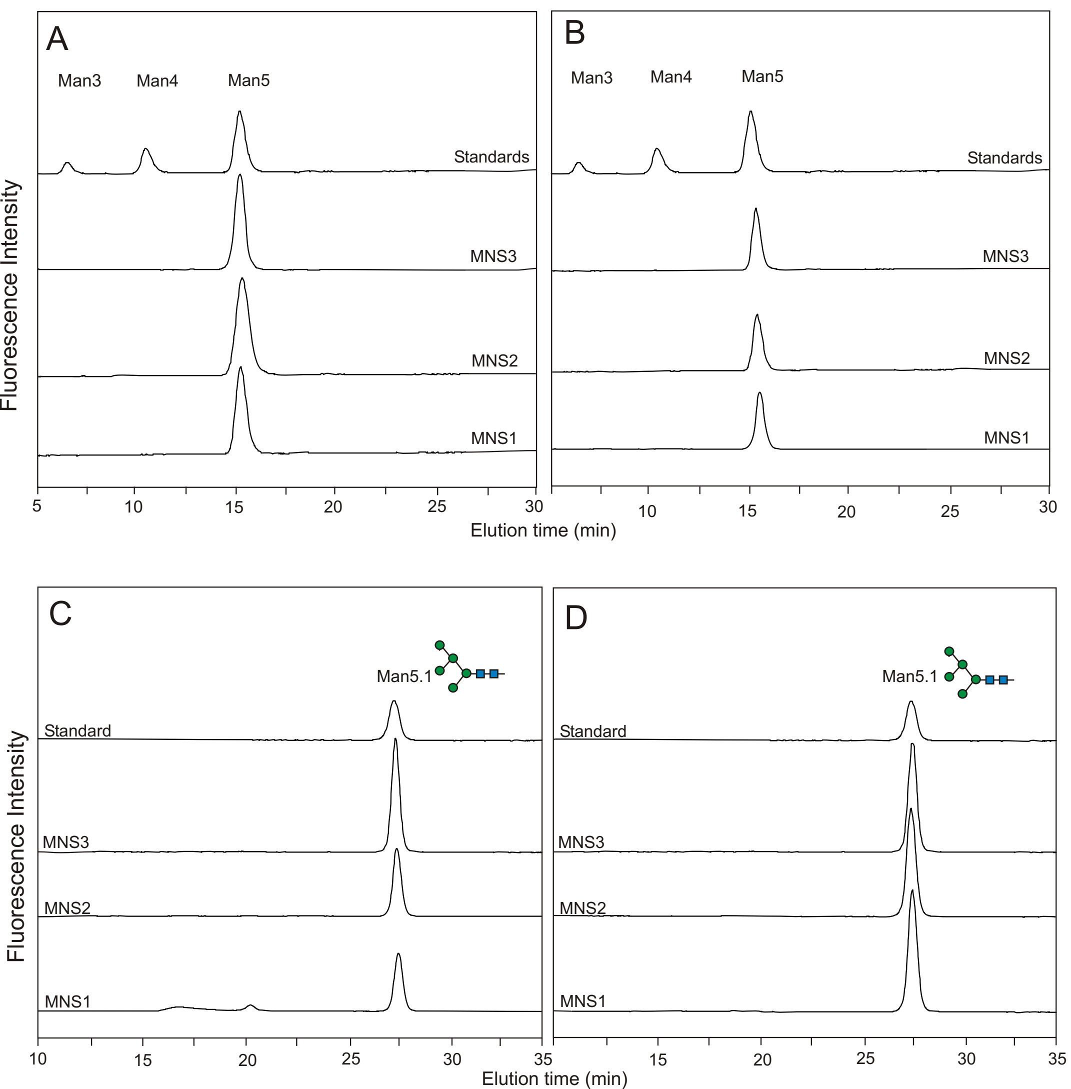

Supplemental Figure 7. The MNS product Man5-PA co-elutes with Man5.1.

Incubation of the substrates $Man_8GlcNAc_2$-PA (**A, C**) and $Man_9GlcNAc_2$-PA (**C, D**) with high amounts of the recombinant enzymes MNS1-3 yielded $Man_5GlcNAc_2$-PA (**A+B**) when analyzed on NP-HPLC. No further trimming of mannoses to $Man_4GlcNAc_2$- or Man_3GcNAc_2-PA occurred. $Man_5GlcNAc_2$-PA peaks were collected and separated on RP-HPLC (**C+D**). All Man5-PA products co-elute with the Man5.1 standard. As other Man5 isomers were shown to have different elution times (Tomiya et al., 1991), this indicates that Man5.1 is the only isomer generated by recombinant MNS proteins.

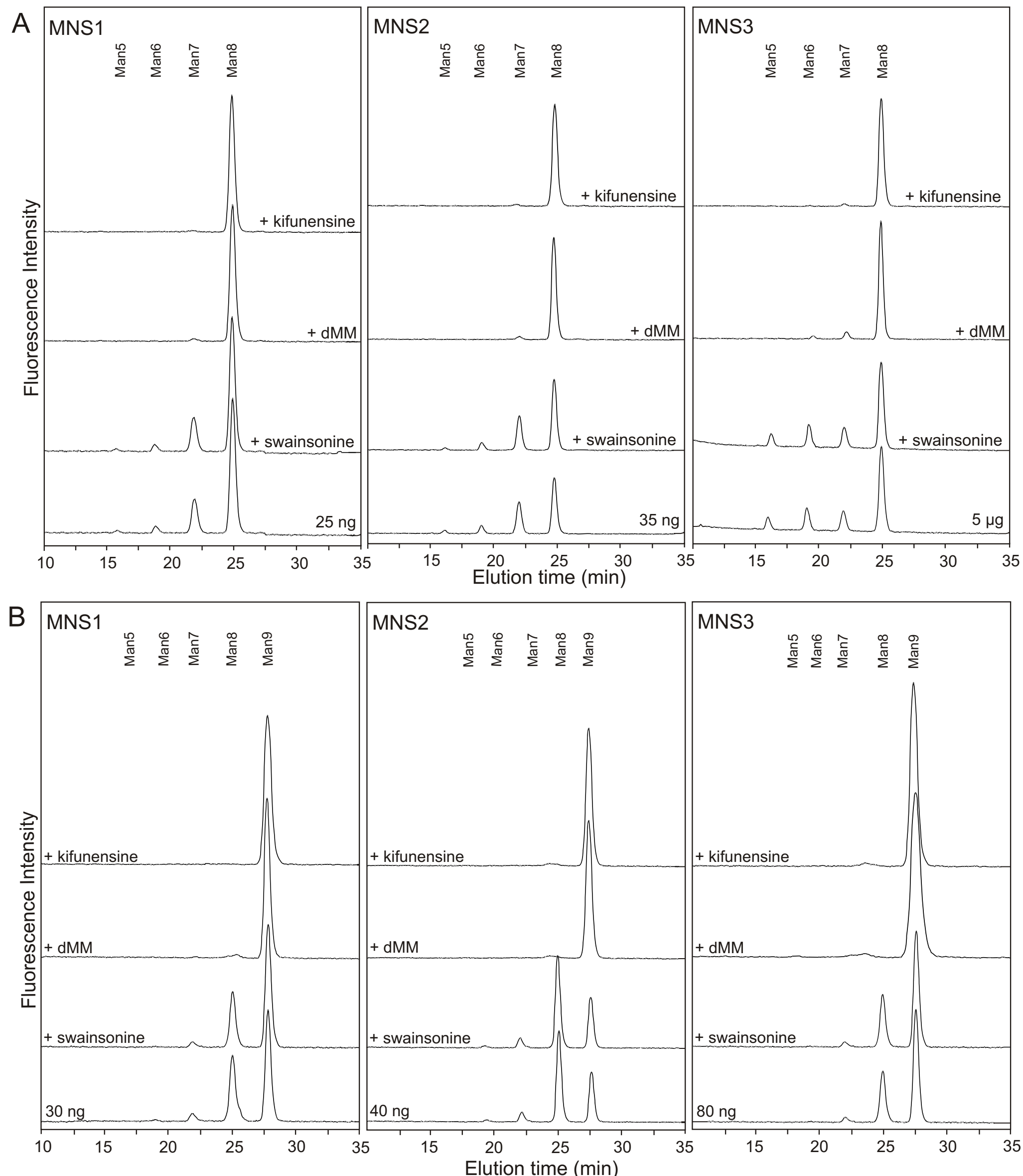

Supplemental Figure 8. **Recombinant MNS proteins are specifically inhibited by kifunensine and 1-deoxymannojirimycin.**

Activity assays with PA-labeled substrates (**A)** $Man_8GlcNAc_2$ and **(B**) $Man_9GlcNAc_2$ were performed in the presence of class I and class II α1,2-mannosidase inhibitors. Assays were performed under conditions where at least 30 percent substrate turnover took place. Briefly, after incubation of the enzymes with a certain amount of inhibitors for 15 min on ice, the samples were handled and analyzed as described in Methods. The class II α1,2-mannosidase inhibitor swainsonine (10 µM) did not affect the enzyme activity of MNS1-3. In contrast, hardly any substrate turnover was seen when the recombinant enzymes were pre-incubated with 1-deoxymannojirimycin (dMM, 100 µM) or kifunensine (1 µM).

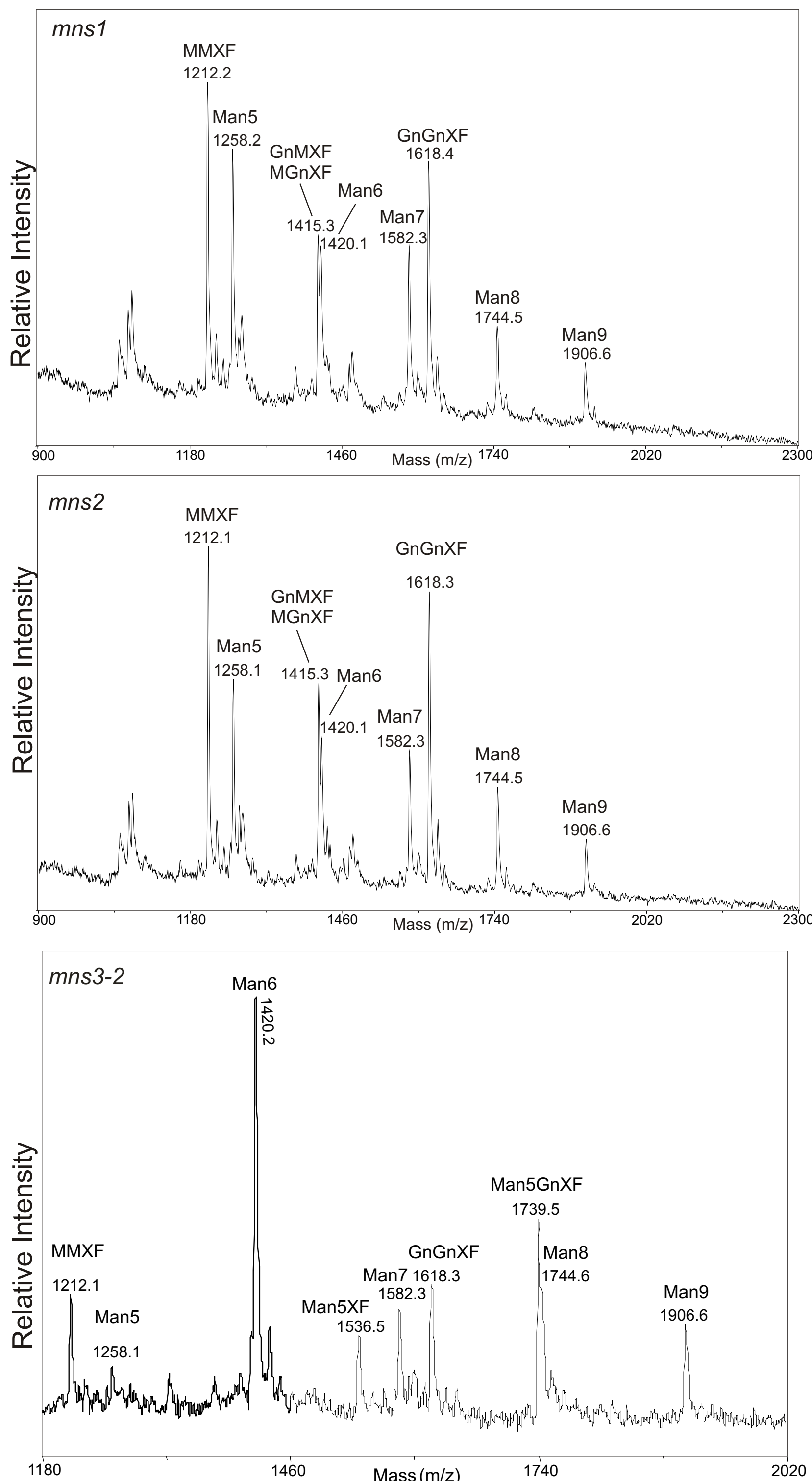

Supplemental Figure 9. N-glycan spectra of leaves of single knockout plants. MALDI-TOF-MS spectra of total N-glycans extracted from leaves of *mns1*, *mns2* and *mns3-2* single mutants. The N-glycan profile of *mns3-1* is essentially the same as that of *mns3-2*.

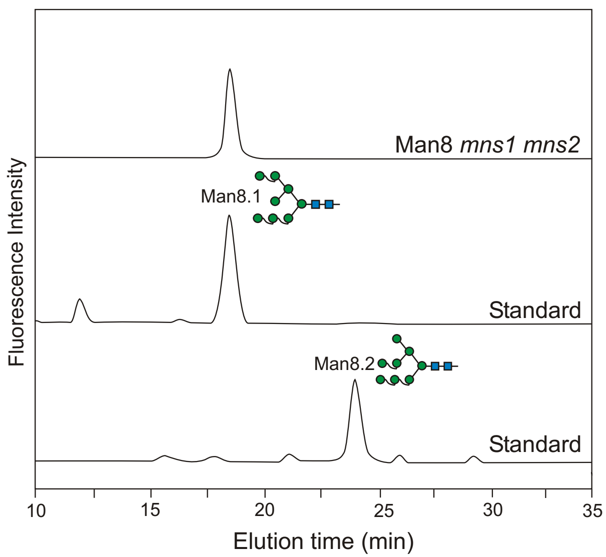

Supplemental Figure 10. The $Man_8GlcNAc_2$ oligosaccheride isolated from glycoprotein extracts of *mns1 mns2* double knockouts co-elutes with Man8.1.

Leaf material of the double knockout was analyzed for total glycans as described previously (Strasser et al., 2004). The prominent $Man_8GlcNAc_2$ peak was isolated by normal-phase HPLC, PA-labeled and analyzed by reverse-phase HPLC. To characterize the isolated peak, two $Man_8GlcNAc_2$ isomers (Man8.1, Man8.2) were used as standards. $Man_8GlcNAc_2$ isolated from the double mutant co-elutes with the Man8.1-PA standard, the isomer lacking the terminal mannose from the b-branch.

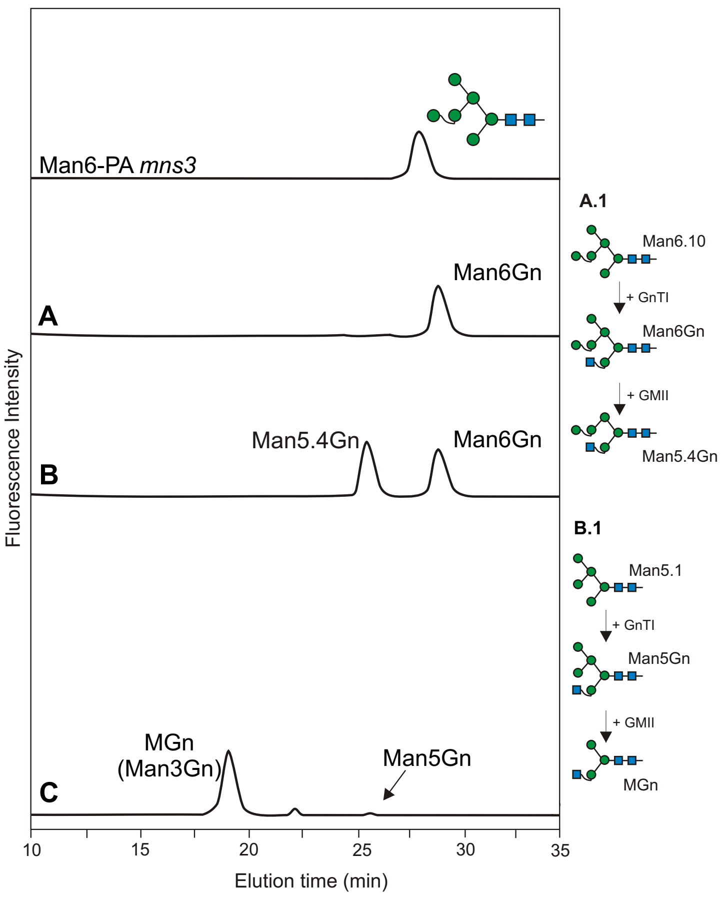

Supplemental Figure 11. The $Man_6GlcNAc_2$ oligosaccharide isolated from *mns3-1* plants is an acceptor substrate for N-acetylglucosaminyltransferase I (GnTI).

$Man_6GlcNAc_2$-PA isolated from *mns3-1* plants (presumably Man6.10) was incubated with recombinant rabbit GnTI and UDP-GlcNAc (5 mM) in the presence of 20 mM $MnCl_2$ in assay buffer (100 mM MES [pH 6.3], 1 mg/ml BSA, 1.25% Triton-100, 1.25 mM DTT, 6.25 µg/ml E-64, 6.25 µg/ml Leupeptin, 2.5 mM PMSF and 25 µM swainsonine) overnight at 37°C. The reaction was stopped by heating at 95°C for 5 min. The product was analyzed by normal-phase HPLC (trace **A**) and the collected Man6Gn peak was incubated with recombinant *Drosophila melanogaster* Golgi α-mannosidase II (GMII) in 50 mM MES buffer (pH 6.0) and 10 µM 2-acetamido-1,2-deoxynojirimycin for 1 h at 37°C. After heating at 95°C for 5 minutes in the presence of 10 µM swainsonine, the sample was again analyzed by normal-phase HPLC (trace **B**). Man6Gn was sensitive to Golgi α-mannosidase II. One mannose residue could be slowly removed resulting in an aberrant Man5Gn-product (Man5.4Gn). No further trimming to MGn occurred, as expected. Digestion of $Man_5GlcNAc_2$-PA (Man5.1) that was treated identically as described above revealed an almost complete removal of two mannose residues resulting in the formation of MGn (trace **C**).

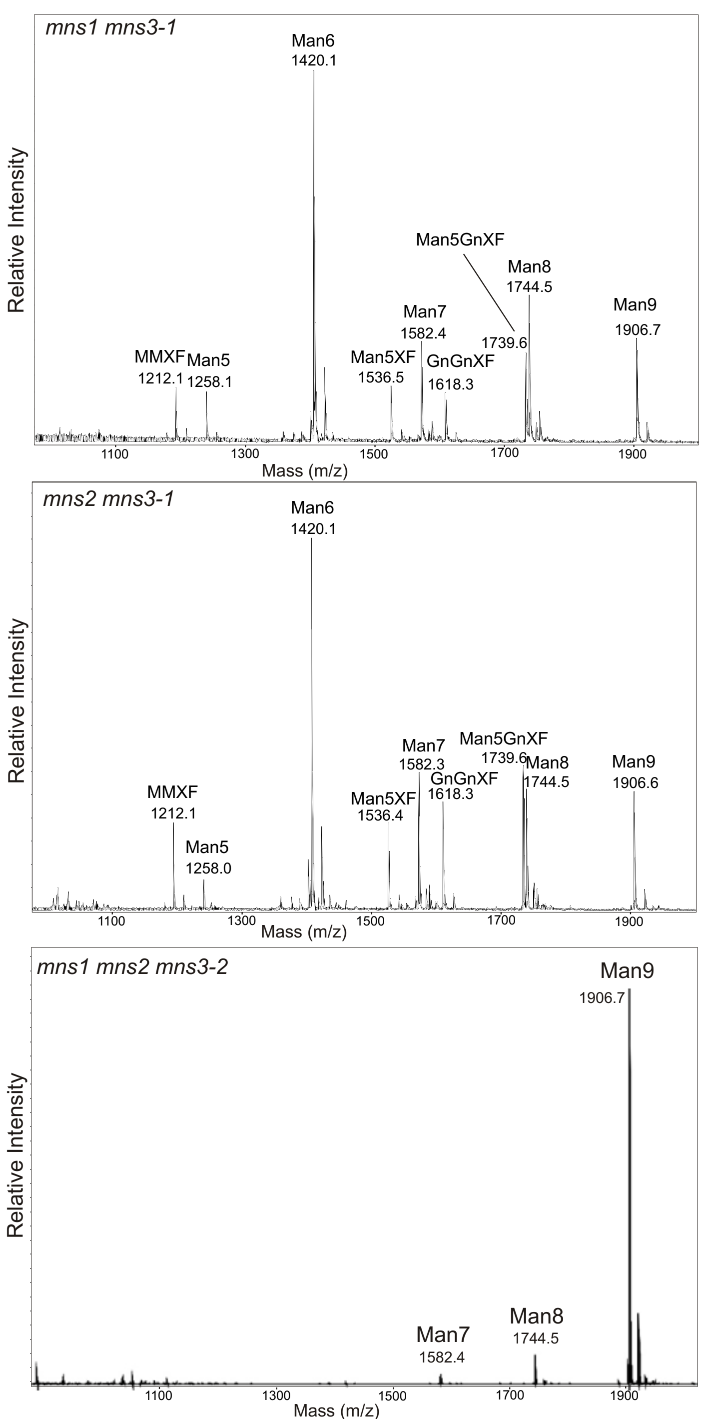

Supplemental Figure 12. N-glycan spectra of leaves of double and triple knockouts (*mns1 mns3-1, mns2 mns3-1, mns1 mns2 mns3-2)*

MALDI-TOF-MS spectra of total N-glycans extracted from leaves of different mutant lines. The N-glycans of *mns1 mns3-1* and *mns2 mns3-1* double mutants are identical to those of the *mns3-1* single mutant (Figure 7A), while *mns1 mns2 mns3-2* shows a predominance of $Man_9GlcNAc_2$ as found in *mns1 mns2 mns3-1* (Figure 7A).

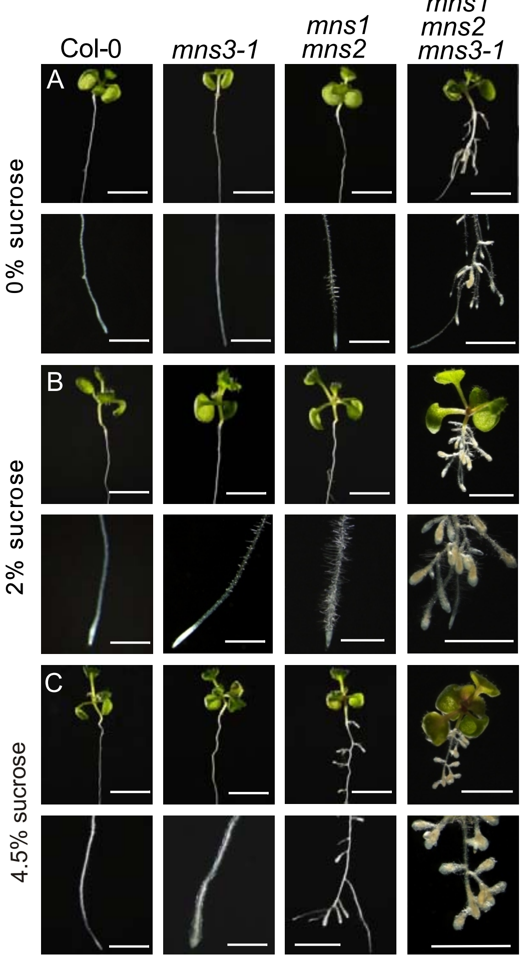

Supplemental Figure 13. ***mns* mutant seedlings are affected by high amounts of sucrose.** After growth of wild-type (Col-0) and *mns* mutant seedlings on MS agar medium with 2% sucrose for five days at 22°C, seedlings were transferred to MS agar plates with 0% sucrose **(A)**, with 2% sucrose (**B)** or with 4.5% sucrose **(C)** and were grown for another six days at 22°C. On plates with 4.5% sucrose, *mns1 mns2* and *mns1 mns2 mns3-1* show a decrease in root length and an increase in radially swollen roots. The *mns3-1* single mutant displays swollen root tips. Scale bar = 5 mm for all images.

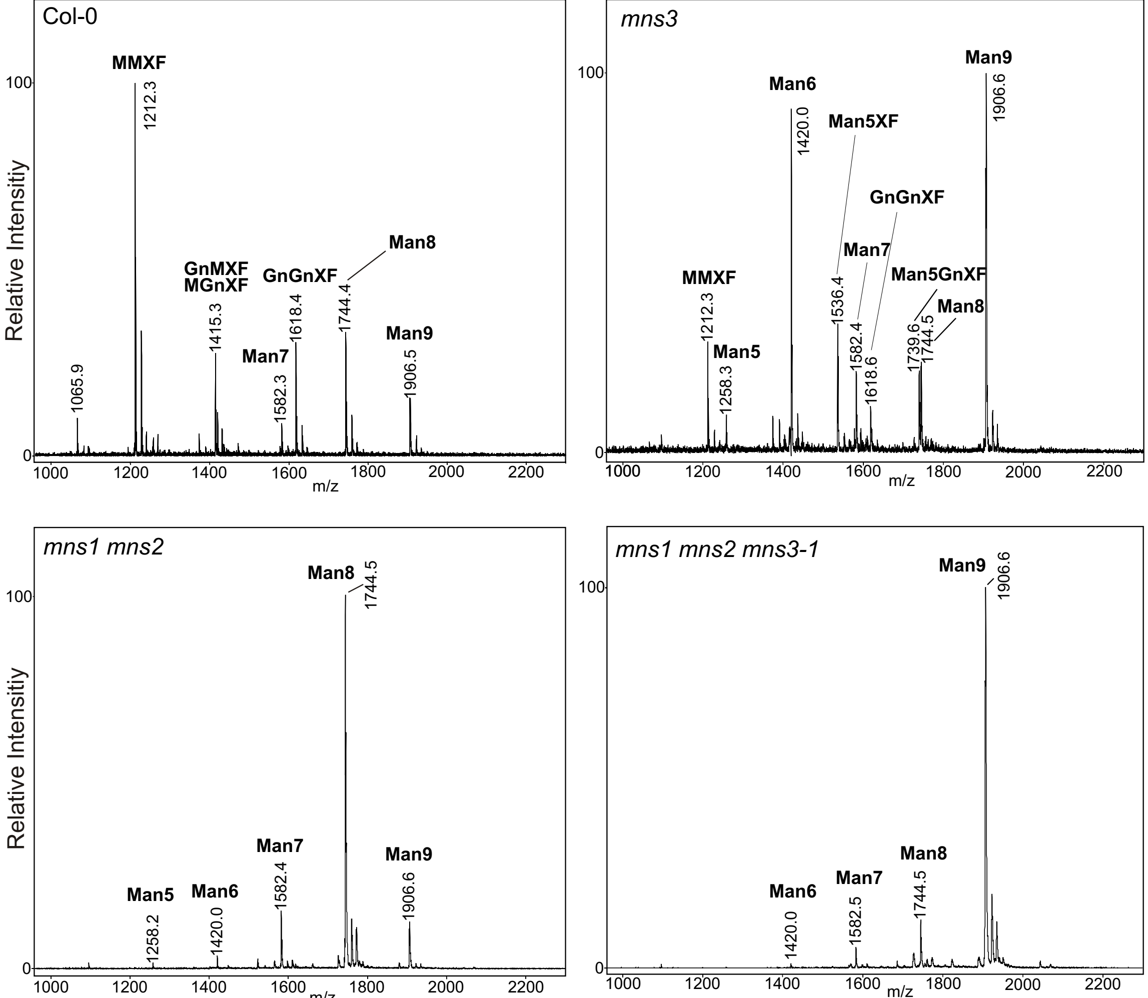

Supplemental Figure 14. N-glycan spectra of roots of wild-type (Col-0), *mns3-1*, *mns1 mns2* and *mns1 mns2 mns3-1 plants.*

Total N-glycans extracted from 500 mg roots of wild-type plants and the *mns* mutants were analyzed by MALDI-TOF-MS. N-glycan patterns are similar to those obtained from leaves in *mns1 mns2* and *mns1 mns2 mns3-1*. An increase in $Man_9GlcNAc_2$ was found in roots of *mns3-1,* which was not present in leaves.

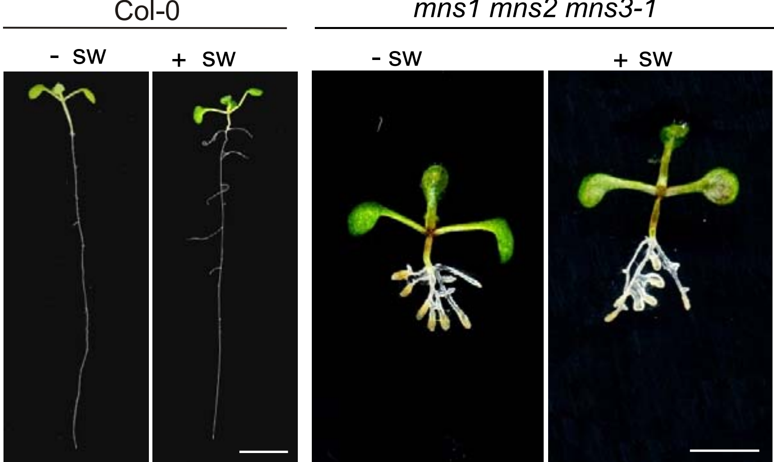

Supplemental Figure 15. Swainsonine has no effect on Col-0 wild-type and *mns1 mns2 mns3-1*.

Col-0 and *mns1 mns2 mns3-1* were grown on MS medium plus 2% sucrose and 100 µM swainsonine for seven days at 22°C. Seedlings do not show any obvious root phenotype when grown on agar plates containing the class II α-mannosidase inhibitor swainsonine. Scale bar = 5 mm.

Supplemental Table 1. Pairwise BLAST alignment of amino acid sequences (see Supplemental Data Set 1). (http://www.ncbi.nlm.nih.gov/BLAST/bl2seq/wblast2.cgi). Identity values (%) are shown.

	At MNS1	At MNS2	At MNS3	At MNS4	At MNS5
At MNS1	-	82	43	30	30
At MNS2		-	43	30	29
At MNS3			-	30	29
At MNS4				-	48
At MNS5					-
Gm MNSI	75	73	42	34	32
Hs ERMNSI	45	44	44	30	31
Hs MNSIA	42	42	35	30	33
Hs MNSIB	44	41	35	30	30
Hs MNSIC	44	42	35	30	29
Hs EDEM1	30	29	30	47	44
Hs EDEM2	32	33	35	46	42
Hs EDEM3	31	31	28	43	43
Sc MNS1	38	36	40	27	28
Sc HTM1	27	27	26	37	34

Supplemental Table 2. Predictions of subcellular localization, number of trans-membrane domains (TMDs), signal anchor or peptide probability and calculation of molecular masses (MW) and isoelectric points (PI).

	Gene ID	Putative subcellular localization[ab,c]	TMD prediction[d,e]	Signal anchor Probability[f]	Signal peptide Probability[f]	MW[g]	PI[h]
At MNS1	At1g51590	SP	1	0.989	0.010	63533.0	6.4
At MNS2	At3g21160	SP	1	0.976	0.023	65137.0	6.4
At MNS3	At1g30000	SP	1	0.993	0.000	69070.0	7.1
At MNS4	At5g43710	SP	1	0.062	0.936	70096.0	4.6
At MNS5	At1g27520	SP	0	0.421	0.578	65708.0	6.4

The predictions and calculations were performed using the following programs: a) http://www.cbs.dtu.dk/services/TargetP/; (SP = secretory pathway); b) http://urgi.versailles.inra.fr/predotar/predotar.html; c) http://hc.ims.u-tokyo.ac.jp/iPSORT/; d) http://www.enzim.hu/hmmtop/; e) http://www.cbs.dtu.dk/services/TMHMM-2.0/; http://www.cbs.dtu.dk/services/SignalP/; f) http://www.arabidopsis.org/; g + h) http://www.arabidopsis.org/, calculated MW (g) and (h) PI.

Supplemental Table 3. **Primer sequences cited in Methods.** Underlined regions represent restriction sites.

Name	Sequence (5′ - 3′)
At1g51590_1F	TGGGTGCAAGGGAACAAAACATC
At1g51590_2R	TTGAAAACCCACTCGTCTAATGAAATAAC
At1g51590_3F	CTGTTTTTGTTGAGTGGGTTGAGAAGAGA
At1g51590_7R	CAAATTCCATTTGAGCAGAAACTGTCT
At1g51590_8R	AGGATCCGGCATCCTTCAGAGTCTTCAAAG
At1g51590_9F	TTCTAGAGATGGCGAGAAGTAGATCGATTA
At1g51590_10R	TATAGGTACCTACCTAAACGTTAATCTGATGACCAA
At1g51590_11F	TATAGCGGCCGCCCGAGAACATGAGGTTGAAGTTT
At1g51590_15R	TCCATGGCTCTTCTCAACCCACTCAACAAA
At1g51590_16F	TGTCGACGTTGCTTTTCATCAATCTACCTAATGA
At3g21160_1F	GAGCGTCACTGAGGATGTGTCTGTCAA
At3g21160_2R	GTCTCAAACATACTGGCAGCATAATCCTT
At3g21160_3F	GGTTTCAATTTCTTCTTCTTCTCCTTTTTC
At3g21160_4R	AGCCCCTCCTACGAATCACACTG
At3g21160_7R	TGGATCCAACATCCTTCAAACTATTGACAG
At3g21160_8F	TTCTAGAGATGGCGAGGAATAAACTTGTAA
At3g21160_9F	TATAGCGGCCGCCCGAGACTACCAGTTTGAAGTTTC
At3g21160_10R	TATAGGTACCTTACTTCTTTGTTATCCGACCATAA
At3g21160_12F	TATATCTAGAATGTCGAAATCTCTACCATATTCAG
At3g21160_13R	TATAGGATCCTTACTTCTTTGTTATCCGACCAT
At3g21160_14F	TGTCGACAATTTTCAAAGAATCAAGATGGAGAGA
At3g21160_15R	TACATGTCAATTCCGACGATCAGATCTGATCTCG
At1g30000_2R	TAACTCCCCTACAAAGACCAGACCT
At1g30000_3F	GGCTTCCACCTCGTTTATCACCT
At1g30000_5F	TTCTAGAATGTCGAAATCTCTACCATATTCAG
At1g30000_6R	TGGATCCTCTTAATTGTCCTTCGTCAGGTGA
At1g30000_8F	TATAGCGGCCGCCGGTCTTAATGAGAAAGGAAAGG
At1g30000_9R	TATAGGTACCTCAGGTGTTTCTTCTTATTGGT
At1g30000_10R	TGGATCCGGTGTTTCTTCTTATTGGTAA
At1g30000_11R	TATAGGATCCTCAGGTGTTTCTTCTTATTGGT
At1g30000_12F	TATATCTAGAATGTCGAAATCTCTACCATATTCAG
At1g30000_14F	TATAGTCGACTCTCTTACATTGGACGAGTACAAGGAGGA
At1g30000_15R	TATACCATGGTCAGATCCCCCCGTTCTAATTGAAG
LBa1	TGGTTCACGTAGTGGGCCATCG
UBQ_5D	AACCCTTGAGGTTGAATCATC
UBQ_5U	CTCCTTCTTTCTGGTAAACGT

Supplemental Methods

Promoter-GUS Fusions

To generate the promoter GUS expression vector pPZP230-GUS the hygromycin expression cassette was amplified from pGreen0129 (Hellens et al., 2000) using primers nos-1/-2 and cloned into the *Kpn*I and *Bam*HI sites of the binary vector pPZP200 (Hajdukiewicz et al., 1994). Subsequently an *Nco*I linker was inserted into the *Sal*I and *Hind*III sites of pPZP230 and the 2 kb uidA-gene fragment containing the CaMV terminator was removed from pSH4 (Holtorf et al., 1995, kindly provided by Holger Bohlmann) and ligated into *Nco*I and *Hind*III sites. For promoter GUS fusions, genomic fragments comprising 1042 bp of 5´ flanking DNA of MNS1, 1621 bp of MNS2 or 873 bp of MNS3 were amplified from wild-type genomic DNA using primers At1g51590-16F/-15R, At3g21160-14F/-15R and At1g30000-14F/-15R and cloned into the *Sal*I and *Nco*I sites of pPZP230-GUS. Col-0 plants were transformed by *Agrobacterium tumefaciens* (strain: UIA143) carrying the GUS expression constructs by the floral dip procedure. Transgenic plants were selected on MS medium containing 20 mg/l hygromycin. Plant material was stained for GUS activity in 0.5 mg/ml X-Gluc in 50 mM $NaHPO_4$ (pH 7.0), 10 mM EDTA, 0.1% Triton X-100 for 18 h at 37°C. After clearing in three changes of 70% ethanol, the plant material was mounted in water. Imaging was done using a Leica MZ FLIII stereomicroscope (Leica, Wetzlar, Germany), equipped with a Leica DC 500 digital camera.

References:

Hajdukiewicz P, Svab Z, Maliga P (1994) The small, versatile pPZP family of Agrobacterium binary vectors for plant transformation. Plant Mol Biol **25:** 989-994.

Hellens R, Edwards E, Leyland N, Bean S, Mullineaux P (2000) pGreen: a versatile and flexible binary Ti vector for Agrobacterium-mediated plant transformation. Plant Mol Biol **42:** 819-832.

Holtorf S, Apel K, Bohlmann H (1995) Comparison of different constitutive and inducible promoters for the overexpression of transgenes in Arabidopsis thaliana. Plant Mol Biol **29:** 637-646.

Neeser, J.-R., Del Vedov, S., Mutsaers, J.H.G.M., and Vliegenthart, J.F.G. (1985). Structural Analysis of the carbohydrate chains of legume storage proteins by 500-MHz 1H-NMR spectroscopy. Glycoconj. J. **2:** 355-364.

Tomiya, N., Lee, Y., Yoshida, T., Wada, Y., Awaya, J., Kurono, M., and Takahashi, N. (1991). Calculated two-dimensional sugar map of pyridylaminated oligosaccharides: elucidation of the jack bean alpha-mannosidase digestion pathway of $Man_9GlcNAc_2$. Anal. Biochem. **193:** 90-100.

Strasser, R., Altmann, F., Mach, L., Glössl, J., and Steinkellner, H. (2004). Generation of *Arabidopsis thaliana* plants with complex N-glycans lacking beta1,2-linked xylose and core alpha1,3-linked fucose. FEBS Lett. **561:** 132-136.